Supporting information

Open-Structured Nanotubes with Three-Dimensional Ion-Accessible Pathways for Enhanced Li^+ Conductivity in Composite Solid Electrolytes

Song Hu[†], *Lulu Du*[†], *Gang Zhang*[†], *Wenyuan Zou*[†], *Zhe Zhu*[†], *Lin Xu*[*†§], *Liqiang Mai*[†§]

†State Key Laboratory of Advanced Technology for Materials Synthesis and Processing, School of Materials Science and Engineering, Wuhan University of Technology, Wuhan 430070, Hubei, P. R. China.

§Foshan Xianhu Laboratory of the Advanced Energy Science and Technology Guangdong Laboratory, Xianhu Hydrogen Valley, Foshan 528200, Guangdong, P. R. China.

*E-mail: linxu@whut.edu.cn

EXPERIMENTAL SECTION

Materials: $LiNO_3$ (>99.99%, Sigma-Aldrich), $La(NO_3)_3 \cdot 6H_2O$ (>99.99%, Aladdin), $Ti(OC_4H_9)_4$ (>99.0%, Aladdin), $LiClO_4$, acetic acid, dimethylformamide (DMF), high molecular weight plyvinylpyrrolidone (HPVP, Mw=1,300,000, Aladdin), low molecular weight plyvinylpyrrolidone (LPVP, Mw=360,000, Aladdin), polyacrylonitrile (PAN, Mw =150,000, Aladdin).

Fabrication of LLTO Nanotubes : Appropriate ratios of $LiNO_3$, $La(NO_3)_3 \cdot 6H_2O$, and $Ti(OC_4H_9)_4$ were dissolved in 16 mL DMF with 4 mL acetic-acid, and added 15 wt% excess $LiNO_3$ for its weight loss during calcination. An appropriate amount of HPVP and LPVP were subsequently added. After rapid stirring for 24 h, a yellow, transparent uniform solution with 13 wt% PVP was obtained. In the process of electrospinning, 10 ml as-obtained precursor solution was pumped into the injection syringe with a stainless steel needle which gauge is 18. In addition, remove the bubbles in the syringe and keep the air humidity below 30%. Then applied a high voltage of 15 KV between needle and collector, which distance is 15 cm. The aluminum foil is tightly wrapped around the rolling collector (50 rpm) to collect the as-spun nanowires. Then, the as-spun nanowires were heated at a different temperature (700-850 °C) for 2 h in air at a heating rate of 5 °C min^{-1}. Similar methods can prepare LLTO NWs, except that the polymer was replaced by 2.4 g high molecular weight PVP. Then electrospinning and sintering steps as above.

For comparison, LLTO nanoparticles have been synthesized via the sol-gel method. $LiNO_3$, $La(NO_3)_3 \cdot 6H_2O$, and $Ti(OC_4H_9)_4$ were dissolved in ethanol solvent. A viscous gel was obtained by stirring at 50 °C for 6 h. After drying, the gel was then calcined at 1000 °C for 4 h in air at a heating rate of 10 °C min^{-1}.

Synthesis of Composite Solid Electrolyte: 0.53 g $LiClO_4$ and an appropriate amount of LLTO NTs (0-15 wt%) were dissolved in 10 mL DMF. After the LLTO NTs have been evenly dispersed by ultrasound, 1.06 g PAN was added to the above solution slowly, and then stirred at 60 °C for 12 h. To obtain composite solid electrolytes, the well-stirred solution was poured into a petridish and dried at 80 °C under vacuum for 12 hours to remove the excess solvent. Finally, the dried film is quickly transferred to the glove box for preservation.

Materials Characterization: SEM images are observed by a JEOL JSM-7100F scanning electron microscope. EDS are obtained by an Oxford IE250 system. Using a JEM-2100F/Titan G2 60–300 transmission electron microscope to collect TEM images. D8 Discover X-ray diffractometer with Cu Kα radiation (λ = 1.054056 Å) with 2θ in the range of 10~80° are used to collect X-ray diffractometer characterizations. Thermo-gravimetric (DTA/TG, STA 449, Netzsch) were conducted to determine the crystal formation of the as-spun fibers and decomposition rate of PVP with different molecular under air atmosphere. Using a Tristar-3020 instrument to test the specific surface area and pore-size distribution of samples and calculated from N_2 adsorption isotherms measured. Stress-Strain curves were tested by Instron 5967.

Electrochemical characterization: Electrochemical impedance spectroscopy (EIS) was tested by assembling a blocking stainless steel|LLTO NTs/PAN CSE|stainless steel cell from 100 Hz to 10^6 Hz with an amplitude of 10 mV via Autolab PGSTAT302N. Arrhenius was obtained by calculating ionic conductivity at a temperature range of 20-80 °C via Autolab PGSTAT302N. The electrochemical stability window was tested by linear sweep voltammetry (LSV) on a lithium|LLTO NTs/PAN CSE|stainless steel cell from 0 to 6.5 V via Autolab PGSTAT302N at a scan rate of 10 mV s^{-1}. The lithium compatibility of lithium|LLTO NTs/PAN CSE|lithium cell was tested by a multichannel battery testing system (Neware CT4008). Constant current density of 0.05 mA cm^{-2} was applied to the battery and the current signal was changed every 30 minutes. This cell is also used to test Current-time profile via Autolab PGSTAT302N.

The rate and cycle performance of Lithium|LLTO NTs/PAN CSE|$LiFePO_4$ was conducted using a multichannel battery testing system (Neware CT4008). $LiFePO_4$ (LFP) is chosen as the cathode material. LFP, Super P and polyvinylidene fluoride (PVDF) are mixed evenly in N-methyl-2-pyrrolidone (NMP) at a mass ratio of 8: 1: 1 to form a uniform slurry, and then coated on a clean aluminum foil. Then the mixture is dried at 70 °C in a vacuum oven for 12 h. The cycle performance of full cells is tested at 0.5 C between 2.8 and 4.0 V. To improve the interface contact, 10 μL (~4 μL cm^{-2}) liquid electrolyte which is 1M of $LiPF_6$ in ethylene carbonate (EC) and dimethyl carbonate (DMC) (EC: DMC with 1:1, vol%) was dropped onto both sides of LLTO NTs/PAN CSE when testing full cell and symmetric battery. $LiNi_{0.8}Co_{0.1}Mn_{0.1}O_2$ (NCM811) is chosen as the high-voltage cathode material. NCM811, Super P and

PVDF are mixed evenly in NMP at a mass ratio of 8: 1: 1 to form a uniform slurry, and then coated on a clean aluminum foil. Then the mixture is dried at 80 °C in a vacuum oven for 12 h. The cycle performance of Li-NCM811 cell is tested at 0.5 C between 3.0 and 4.3 V. All of the cells were assembled with 2016 coin-type cells in glove box and tested at room temperature.

Supplementary Text

The XRD patterns shown in Figure S2 indicate that the diffraction peaks of LLTO nanotubes calcined at different temperatures could be indexed to a perovskite structure with the tetragonal P4/mmm space group, while the impurity of $La_2Ti_2O_7$ could be detected in LLTO nanotubes and nanowires. In addition, the impurity of $LiTi_2O_4$ could be found in nanotubes.[1, 3]

In Figure S6, the weight loss before 350 °C could be attributed to the removal of DMF, due to its fairly high boiling point of 150 °C and its strong affinity with the nitrile group of PAN.[3] In addition, we can observe rapid weight loss at 358 °C which is mainly due to the dehydrogenation of PAN. The decomposition temperature of PAN reduced slightly by the introduction of LLTO nanotubes. When the temperature exceeds 550 °C, the LLTO NTS phase is obvious in LLTO NTS /PAN CSE.

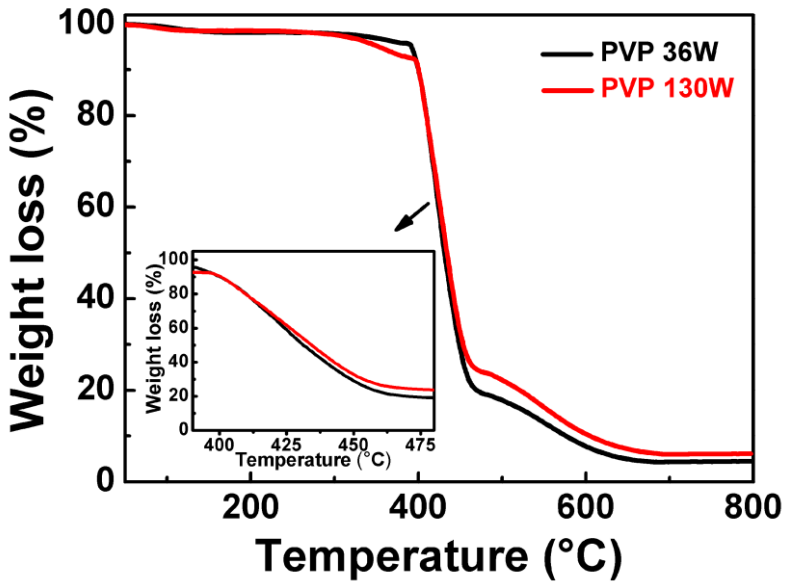

Figure S1. TGA curves of the PVP with high molecular weight (Mw= 1, 300, 000) and low molecular weight (Mw= 360, 000) and the inset shows TGA cures of PVP between 400-475 °C.

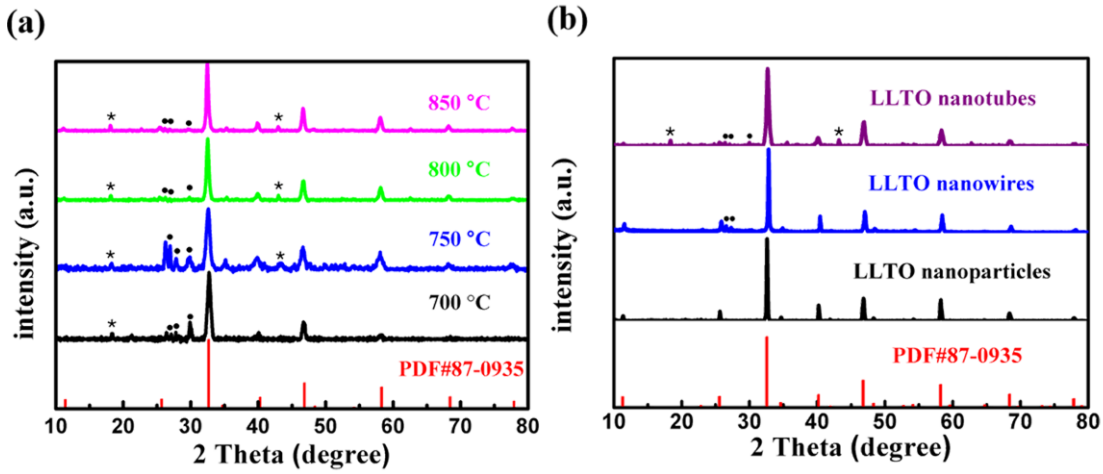

Figure S2. a) XRD patterns of as-spun nanowires calcined at 700, 750, 800 and 850 °C. b) XRD patterns of synthesized LLTO nanotubes, nanowires and nanoparticles. (●) $La_2Ti_2O_7$, (★) $LiTi_2O_4$.

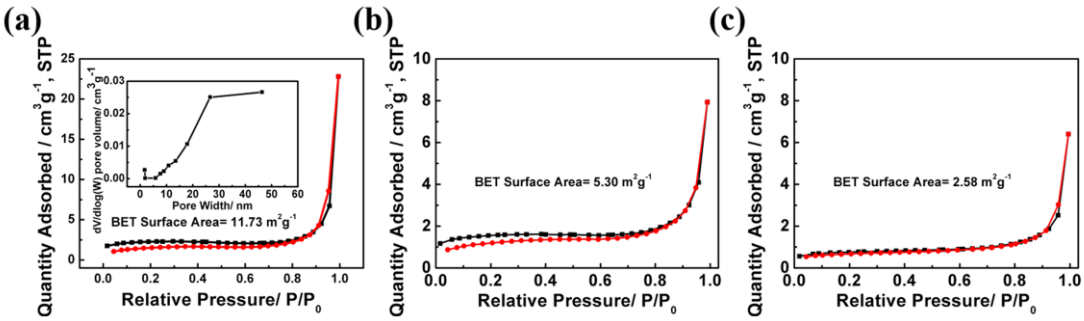

Figure S3. BET surface area of a) LLTO nanotubes, b) LLTO nanowires and c) LLTO nanoparticles (the inset in (a) shows pores distribution of LLTO nanotubes).

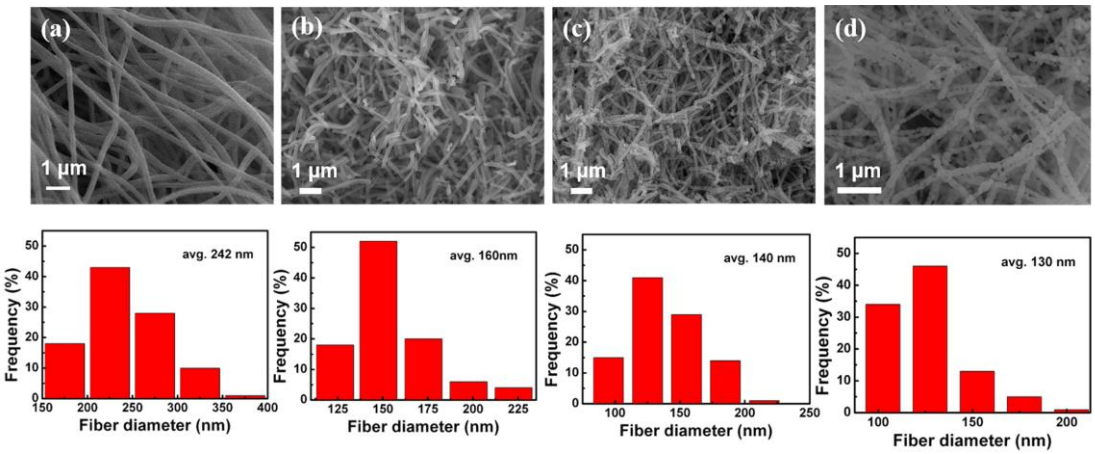

Figure S4. The average diameters and SEM images of (a) as-spun nanowires and LLTO NTs calcined at (b) 700, (c) 800 and (d) 850 °C for 2 h.

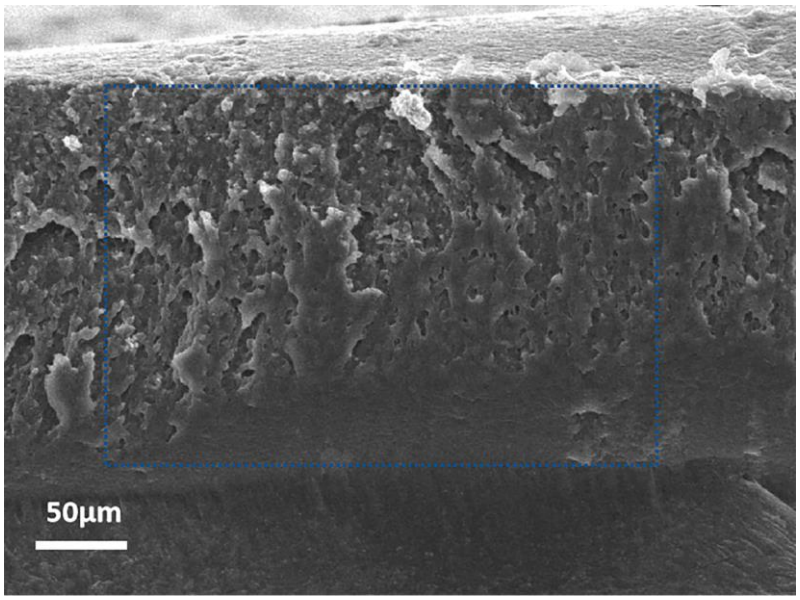

Figure S5. Cross-section SEM image of the 10LLTO NTs/PAN CSEs.

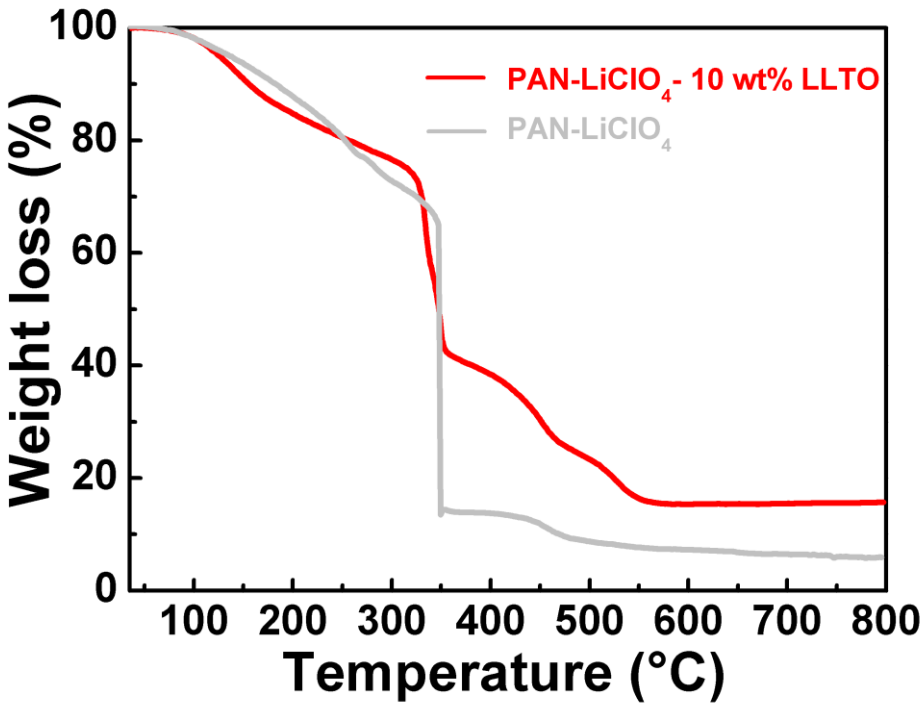

Figure S6. TGA curves of the 10LLTO NTs/PAN CSEs and bare PAN solid electrolytes.

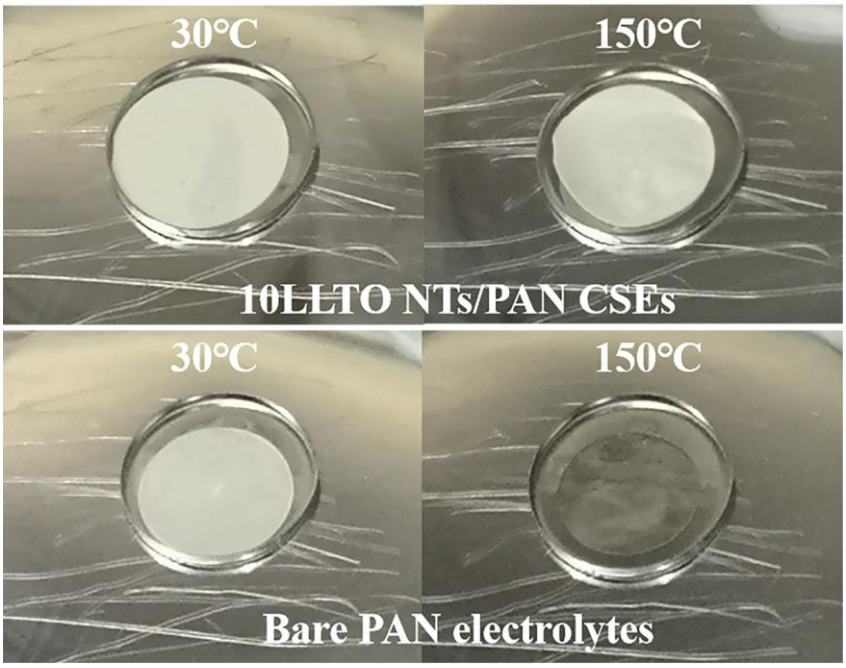

Figure S7. Thermal shrinkage optical images of 10LLTO NTs/PAN CSEs and bare PAN solid electrolytes heating at 30 °C and 150 °C.

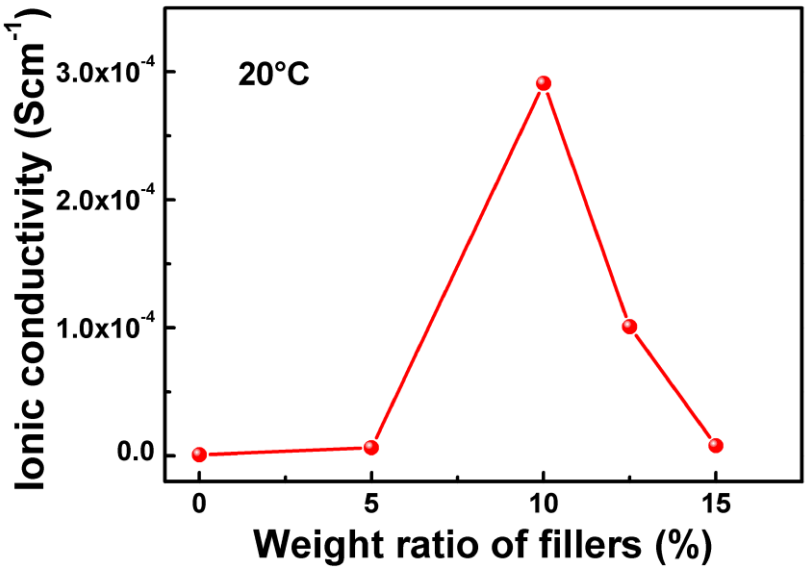

Figure S8. Ionic conductivity of the LLTO NTs/PAN CSEs with different weight ratio of LLTO NTs at 20 °C.

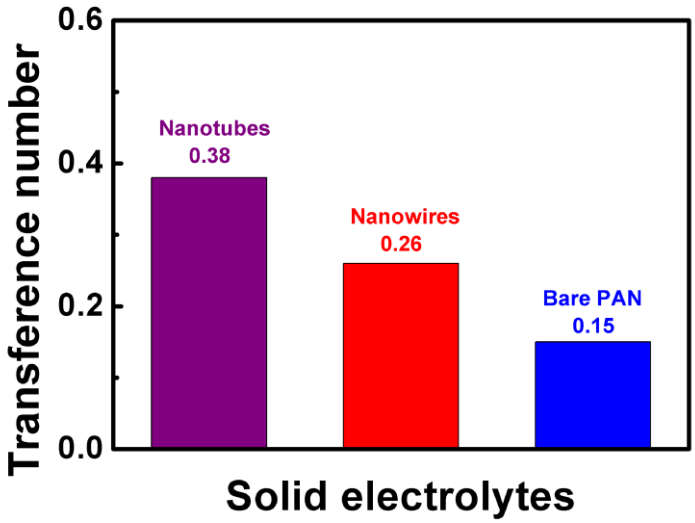

Figure S9. Li ion transference number of bare PAN solid electrolytes and PAN-based composite solid electrolytes with LLTO nanotubes and LLTO nanowires as fillers.

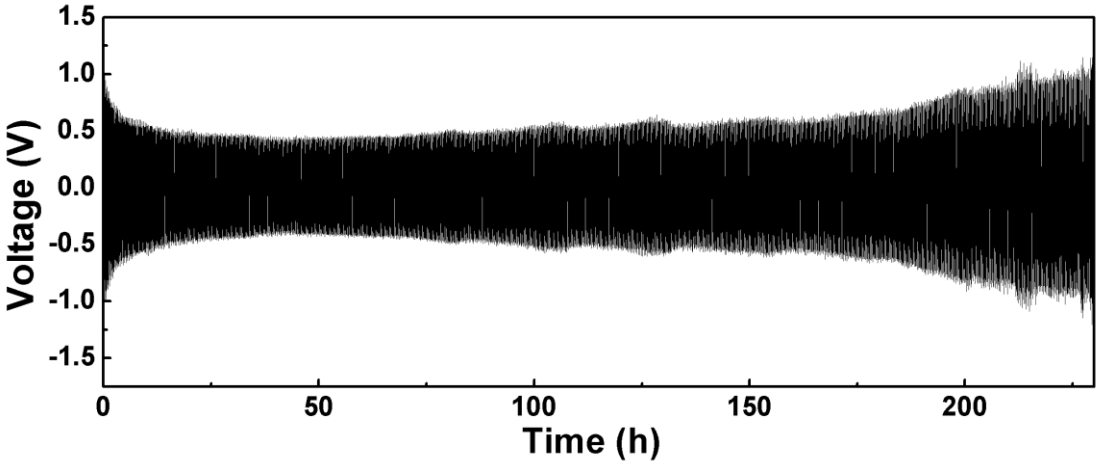

Figure S10. Bare PAN solid electrolytes voltage profile of the continued lithium plating/stripping cycling with a current density of 0.05 mA cm^{-2} at room temperature.

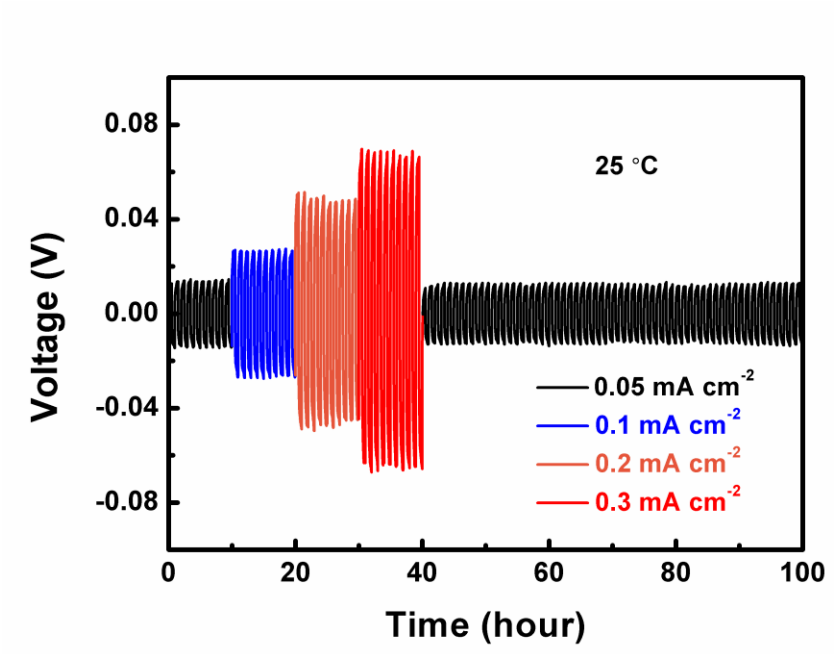

Figure S11. Galvanostatic cycling of a symmetric cell Li/LLTO NTs/PAN CSE/Li under different current densities.

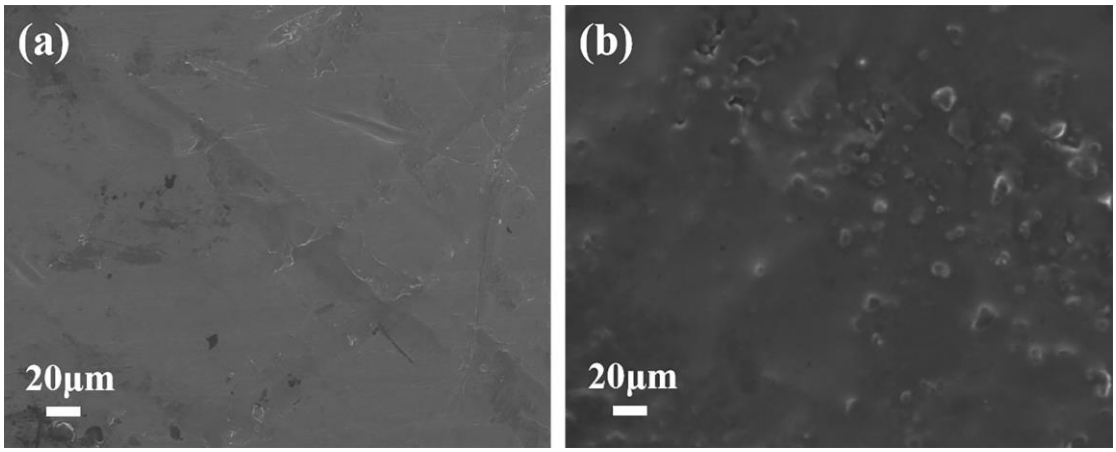

Figure S12. SEM images of the (a) pristine Li metal and (b) Li surface obtained from lithium symmetrical cell assembled with LLTO NTs/PAN CSE after 1000 h cycling at 0.05 mA cm^{-2} and 25 °C.

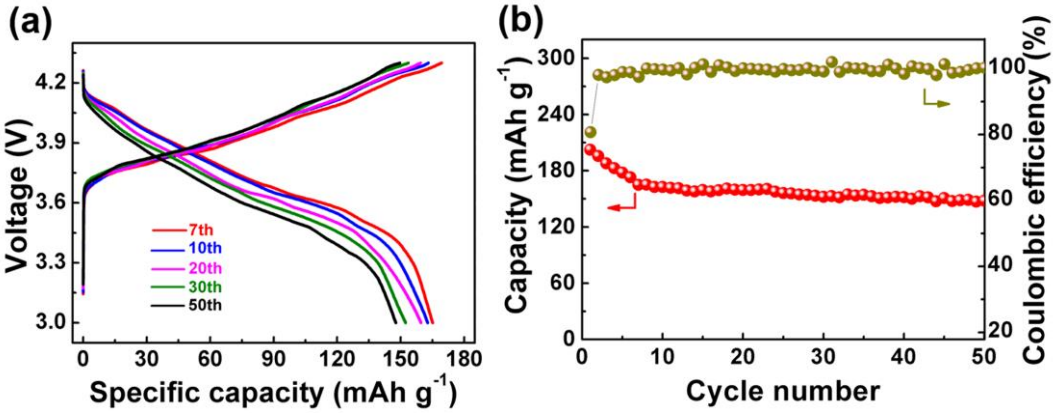

Figure S13. (a) Typical charge/discharge profiles at a rate of 0.5 C, b) cycling stability with Coulombic efficiency under 0.5 C of Li/LLTO NTs/PAN CSE/NCM811 solid-state battery.

Table S1. Comparison between the ionic conductivity of CSEs with different structure of LLTO.

Type of electrolyte	Ionic Conductivity	Temperature	Reference
3D-LLTO/PEO	1.8×10^{-4} S cm^{-1}	25°C	(1)
LLTO nanofiber/PEO	2.4×10^{-4} S cm^{-1}	25°C	(2)
LLTO nanowire/PAN	2.4×10^{-4} S cm^{-1}	25°C	(3)
LLTO nanowire/PEO	3.1×10^{-6} S cm^{-1}	25°C	(4)
LLTO nanoparticle/PEO	2.8×10^{-3} S cm^{-1}	65°C	(5)

Supporting Information Reference

(1) Wang, X.; Zhang, Y.; Zhang, X.; Liu, T.; Lin, Y. H.; Li, L.; Shen, Y.; Nan, C. W., Lithium-Salt-Rich PEO/$Li_{0.3}La_{0.557}TiO_3$ Interpenetrating Composite Electrolyte with Three-Dimensional Ceramic Nano-Backbone for All-Solid-State Lithium-Ion Batteries. *ACS Appl. Mater. Interfaces* **2018,** *10*, 24791-24798.

(2) Zhu, P.; Yan, C.; Dirican, M.; Zhu, J.; Zang, J.; Selvan, R. K.; Chung, C.-C.; Jia, H.; Li, Y.; Kiyak, Y.; Wu, N.; Zhang, X., $Li_{0.33}La_{0.557}TiO_3$ Ceramic Nanofiber-Enhanced Polyethylene Oxide-Based Composite Polymer Electrolytes for All-Solid-State Lithium Batteries. *J. Mater. Chem. A.* **2018,** *6*, 4279-4285.

(3) Liu, W.; Liu, N.; Sun, J.; Hsu, P. C.; Li, Y.; Lee, H. W.; Cui, Y., Ionic Conductivity Enhancement of Polymer Electrolytes with Ceramic Nanowire Fillers. *Nano Lett.* **2015,** *15*, 2740-2745.

(4) He, K. Q.; Zha, J. W.; Du, P.; Cheng, S. H.; Liu, C.; Dang, Z. M.; Li, R. K. Y., Tailored High Cycling Performance in a Solid Polymer Electrolyte with Perovskite-Type $Li_{0.33}La_{0.557}TiO_3$ Nanofibers for All-Solid-State Lithium Ion Batteries. *Dalton Trans.* **2019,** *48*, 3263-3269.

(5) Milian Pila, C. R.; Cappe, E. P.; Mohallem, N. D. S.; Alves, O. L.; Aguilar Frutis, M. A.; Sánchez-Ramírez, N.; Torresi, R. M.; León Ramírez, H.; Laffita, Y. M., Effect of the LLTO Nanoparticles on the Conducting Properties of PEO-Based Solid Electrolyte. *Solid State Sci.* **2019,** *88*, 41-47.